Host porphobilinogen deaminase deficiency confers malaria resistance in *Plasmodium chabaudi* but not in *Plasmodium falciparum* or *Plasmodium berghei* during intraerythrocytic growth

Cilly Bernardette Schnider[1,2,a]

Bernardette.schnider@gmail.com

Hao Yang[1]

Hao.yang@anu.edu.au

Lora Starrs[1]

Lora.starrs@anu.edu.au

Anna Ehmann[1,b]

Anna.ehmann@mater.uq.edu.au

Farid Rahimi[3]

farid.rahimi@anu.edu.au

Elena Di Pierro[4]

Elena.dipiero@unimi.it

Giovanna Graziadei[4]

Giovanna.graziadei@yahoo.it

Kathryn Matthews[5]

Kat.matthews@deakin.edu.au

Tania De Koning-Ward[5]

Tania.dekoning-ward@deakin.edu.au

Denis C. Bauer[6]

Denis.bauer@csiro.au

Simon J. Foote[1]

Simon.foote@anu.edu.au

Brendan J. McMorran[1,c]

Corresponding author

Brendan.mcmorran@anu.edu.au

Gaetan Burgio[1,c]

Corresponding author

Gaetan.burgio@anu.edu.au

[1] Department of Immunology and Infectious Disease, John Curtin School of Medical Research, The Australian National University, Canberra, ACT 2601, Australia.

[2] Department of Biomedical Sciences Faculty of Medicine and Health Sciences, Macquarie University, NSW 2109 Australia.

[3] Research School of Biology, The Australian National University, Canberra, ACT 2601, Australia.

[4] Fondazione IRCCS Ca' Granda - Ospedale Maggiore Policlinico, Rare Diseases Center, Internal Medicine Unit, Department of Medicine and Medical Specialties, Via Francesco Sforza, 35, 20122 Milan, Italy.

[5] School of Medicine, Deakin University, Warn Ponds, VIC 3216, Australia

[6] Health and Biosecurity, CSIRO, Sydney, NSW 2113, Australia.

[a] Current address: Institute of Cell Biology, University of Bern, Bern, Switzerland.

[b] Current address: Mater Research, University of Queensland, South Brisbane , QLD 4101, Australia

[c] Contributed equally to this work

ABSTRACT

Background: The selective pressure imparted by intraerythrocytic infection with *Plasmodium* parasites, the causative agents of malaria has led to many mutations in erythrocytic genes that confer host resistance. Identification and characterization of mutations affecting host resistance to *Plasmodium* infection enables a deeper understanding of host–pathogen interactions and potentially new ways by which to prevent infection.

Methods: Using ENU-induced mutagenesis, and screening for erythrocyte abnormalities and resistance to *Plasmodium chabaudi* infection, we identified a novel nonsense mutation in the gene encoding porphobilinogen deaminase (PBGD) in mice.

Results: Heterozygote *Pbgd* mice exhibited microcytosis and 25% reduction in cellular PBGD activity, but were healthy otherwise. When challenged with blood-stage *P. chabaudi*, the heterozygotes were significantly protected against infection, showed reduced parasite growth, and had a survival advantage. The mutation did not affect erythrocyte susceptibility to parasite invasion. Instead, the mechanism of underlying resistance to infection involved intraerythrocytic parasite death and reduced propagation of viable parasites. This was not observed when *P. falciparum* was cultured in erythrocytes from patients with acute intermittent porphyria (AIP), who have low PBGD levels or with *P. berghei* infection in *Pbgd* deficient mice. Furthermore, the growth capacity of PBGD-null *P. falciparum* and *P. berghei* parasites, which grew at the same rate as their wild-type counterparts in normal erythrocytes, was not reduced in the AIP erythrocytes or *Pbgd*-deficient mice.

Conclusions: Our results suggest that PBGD deficiency confers resistance to infection with *P. chabaudi* during the blood-stage of infection and erythrocytic or parasite PBGD is likely to be dispensable for parasite maturation.

Keywords: Plasmodium, host, porphobilinogen deaminase, porphyria, erythrocytes, N-ethyl-N-nitrosourea

BACKGROUND

Symptomatic and lethal stages of malaria occur when *Plasmodium* parasites invade and replicate within erythrocytes. The ongoing relationship between parasite and host, spanning primordial vertebrates and human evolutionary history, has exerted significant selective pressures on human populations. This has manifested as polymorphisms and mutations that produce altered erythrocytic proteins, many of which are associated with host resistance to infection. These include hemoglobinopathies and deficiencies in cytoskeletal proteins or enzymes that are highly expressed in erythrocytes; they act either directly by impeding parasite invasion or growth, or indirectly on host immune responses and parasite clearance [1-4]. By virtue of its parasitic lifestyle during the blood-stage of the disease, *Plasmodium* scavenges erythrocyte enzymes, including protein kinases, cellular redox regulators, and those involved in heme biosynthesis [5-9]. Depriving parasites of such host enzymes may also contribute also to resistance to *Plasmodium* infection and facilitate identifying novel antimalarial therapeutics as reported in model systems [10, 11].

Heme is an essential cofactor in many proteins and enzymes, for example in hemoglobin as a carrier of oxygen and carbon dioxide. The canonical heme biosynthetic pathway uses eight enzymes, which catalyze conversion of glycine and succinyl-CoA into protoporphyrin, and subsequent Fe^{2+} incorporation. Heme biosynthesis is essential in humans and deficiency of any of the synthetic enzymes is lethal. However, mutations that depress enzyme production or activity are known and cause porphyria. Characteristic symptoms of porphyria may include mild to severe

126 skin photosensitivity, liver malfunction and neurological problems, and are caused by
127 build-up of toxic porphyrin precursors and their derivatives. Specific symptoms and
128 disease severity depend on the composition and levels of these molecules, which in
129 turn are determined by enzyme activity and responsible mutations.
130 *Plasmodium* has a canonical heme biosynthesis pathway [12]. Interestingly,
131 essentiality of the pathway differs depending on the parasite life-cycle stage. *P.*
132 *berghei* made genetically deficient in either the first (δ-aminolevulinic acid synthase;
133 ALAS) or last (ferrochelatase; FC) enzyme of the pathway are not viable in the
134 mosquito stages, but propagate in the mouse bloodstream and cause symptoms that
135 are indistinguishable from those by wild-type parasites [12, 13]. Similarly, the growth
136 of *P. falciparum* cultured in human erythrocytes is not affected by deletion of FC, or
137 two other pathway enzymes, porphobilinogen deaminase (PBGD) and
138 coproporphyrinogen oxidase [12, 14]. These enzyme-deficient parasite lines may
139 acquire heme directly from the degradation of host hemoglobin, based on the
140 observation that no heme is synthesized in FC-deficient *P. falciparum* [12].
141 Additional parasite heme-acquisition mechanisms involving co-opting of the host
142 heme-biosynthetic enzymes that participate in *de novo* synthesis have also been
143 reported [5, 9, 15]. Even though heme biosynthesis is restricted to erythroid
144 progenitors, mature erythrocytes contain detectable amounts of active enzymes [16-
145 18], including PBGD, which is biosynthetically active in mature erythrocytes [14].
146 Previously, we showed that the growth of both *P. chabaudi* and *P. falciparum* was
147 significantly perturbed in mouse and human erythrocytes with reduced levels of FC
148 (erythropoietic protoporphyric erythrocytes). In contrast, *P. falciparum* grew
149 normally in X-linked dominant protoporphyric erythrocytes, which have normal
150 levels of FC, but elevated porphyrin precursors. Collectively, this indicated that,

rather than any non-specific effects caused by FC insufficiency affecting on the parasite, *Plasmodium* has a specific requirement for host FC to sustain its intraerythrocytic growth in erythrocytes [19]. However, here we provide evidence that *Plasmodium* do not rely on erythrocytic PBGD to grow. We found that PBGD insufficiency, both in mice carrying a novel mutation in the gene encoding *Pbgd*, and in human erythrocytes from acute intermittent porphyria (AIP) patients, does not result in impaired parasite growth.

METHODS

Ethics statement

Blood sampling and experimental procedures involving patients were performed in accordance with the 1983 revision of the Declaration of Helsinki. The study was approved by the Ethical Committee of Fondazione IRCCS Ca' Granda, Ospedale Maggiore Policlinico, Milan, Italy (Project Number 246_2015) and The Australian National University Human Research Ethics Committee (2014/765).

All procedures involving animals conformed to the *Australian code of practice for the care and use of animals for scientific purposes* by the Australian National Health and Medical Research Council and were approved by Macquarie University Animal Ethics Committee (Project Numbers: ARA 2012/017 and 2012/019), the Australian National University Animal Experimentation Ethics Committee (2014/53) and Deakin University animal ethics committee (Project Number G37-2013).

Animals

Mice were bred and housed under specific pathogen-free conditions. Mice were housed under controlled temperature (21°C) with a 12:12 h light–dark cycle and fed a

176 diet of Rat and Mouse Premium Breeder chow (Gordons Specialty Feeds, Glen
177 Forest, WA, Australia). Seven-week-old SJL/J male mice were injected
178 intraperitoneally (IP) with 150 mg/kg of *N*-ethyl-*N*-nitrosourea (ENU) at one-week
179 intervals. Mutagenized G0 mice were crossed with background SJL/J mice. G1s were
180 bled after seven weeks for blood analysis. The G1 58155 founder displayed a mean
181 corpuscular volume that was two standard deviations smaller than average; it was
182 crossed with SJL/J and resulting G2s were used in further experiments. For each
183 experimental procedure, heterozygous *Pbgd*^{MRI58155} mice were compared to their wild-
184 type littermates and housed together, up to five animals per cage (Green Line IVC,
185 Tecniplast, PA). Sample sizes were chosen based on statistical power calculations to
186 limit the number of animals used. For generating *P. berghei Pbgd*-knockout parasites,
187 6–8-week-old Balb/c mice were used.
188
189 **Mouse phenotyping**
190 Complete blood cell counts were obtained using an ADVIA® 2120 hematology
191 system. Erythroid progenitors were examined by staining the bone-marrow-derived
192 cells from mutant and wild-type mice with anti-TER119 and anti-CD44
193 (eBioscience). Cells were analyzed on a BD FACSARIA™-II flow cytometer,
194 recording 10,000 events per sample. Populations were gated as described [20].
195 Cytokine Flexset assays (BD Bioscience) were used to measure plasma cytokine
196 concentrations according to the manufacturer's instructions.
197 Erythrocyte life span was determined by following intravenous administration of 1
198 mg of NHS-biotin-ester dissolved in 0.9% (w/v) saline, and blood sampling by tail-
199 snipping each day for seven days, and staining with anti-TER119 and anti-CD71
200 (eBioscience). Cells were suspended in phosphate-buffered saline (PBS; 10 mM

sodium phosphate, 2.7 mM KCl, 140 mM NaCl, pH 7.4) containing 1% (w/v) BSA solution containing 10^8 counting beads/µL, and the number of $TER119^+$ $CD71^-$ cells calculated per bead.

Hepatic and splenic iron levels were measured in tissues dried at 45 °C for 48 h and then digested in a 10% hydrochloric acid/10% trichloroacetic acid (TCA) solution for 48 h at 65 °C. Samples were centrifuged (10000×*g* for 5 min); 200 µL of supernatant was added to 1 mL of 1,10-phenanthroline monohydrate solution and incubated for 15 min at ~23 °C. After incubation, absorbance was measured at $\lambda = 508$ nm.

Erythrocytic osmotic fragility was determined by incubating blood samples diluted 1:100 in NaCl solutions ranging from 0 to 160 mM. After 30 min at 37 °C, samples were centrifuged and absorbance of the supernatant measured at $\lambda = 545$ nm. Percentage lysis was calculated by comparison to 100% lysis in pure water.

Whole-exome sequencing

DNA from two phenodeviant MRI58155 mice was isolated using a Qiagen DNeasy Blood and Tissue Kit (Hilden, Germany). DNA (≥10 µg) was prepared for paired-end genomic library sequencing using a kit from Illumina (San Diego, CA). Exomes were enriched using the Agilent SureSelect kit. Samples were sequenced using a Hiseq 2000 platform. Variants were identified and filtered as described [21]. Briefly, we mapped the short sequence tags (reads) on the mouse genome (mm10/NCBI38) using BWA V0.61 [22] and BOWTIE2 [23]. Nucleotide variants were identified using SAMTOOLS V0.1.19 [24] and GATK [25]. Through our variant-filtration process, we retained those variants that are "common" and "private" to the two mutants, and not shared by other SJL/J mice or previously sequenced ENU-mutant mice. Remaining variants were annotated using ANNOVAR [26].

226

227 **PBGD assay**

228 Whole-blood samples were collected by cardiac puncture, erythrocytes purified and
229 duplicate samples from five wild-type and five heterozygous mice were analyzed for
230 PBGD activity. Whole blood samples were centrifuged at 1500×*g* for 10 min. The
231 plasma and buffy coat were removed. To obtain hemolysates, erythrocytes were
232 washed thrice in PBS then diluted 50-fold in the assay buffer (50 mM Tris containing
233 0.2% Triton X-100, 20 mM citric acid, pH 8.2), incubated at 56 °C for 15 min, and
234 finally cooled on ice. Aliquots (125 µL) of the hemolysates were mixed with 245 µL
235 assay buffer containing 175 µM porphobilinogen (Sigma Aldrich, Castle Hill,
236 Australia) and incubated at 37 °C for 60 min. The reaction was terminated by adding
237 375 µL 12.5% TCA, and oxidation of uroporphyrinogen III (URO III) to URO I was
238 allowed to occur for 30 min at ~23 °C. After centrifugation (1000×*g*, 5 min), 200 µL
239 of clarified supernatant was transferred to brown glass vials, stored at 4 °C, and
240 subjected to ultrahigh-performance liquid chromatography (UHPLC) within 72 h.
241 Samples from each mouse were assayed and analyzed twice in separate reactions. The
242 UHPLC system consisted of a Dionex UltiMate™ 3000 in line with a fluorescence
243 FLD-3400 detector. A Hypersil Gold C18 column (1.9 µm particle size, 50 × 2.1 mm
244 internal diameter; Thermo Fisher Scientific, Australia) was used for elution. The
245 mobile phase consisted of 9% (v/v) acetonitrile in 1 M ammonium acetate–acetic acid
246 buffer, pH 5.16 (solvent A), and 10% acetonitrile (v/v) in methanol (solvent B) [27-
247 29]. The elution program was 0% B (100% A) for initial 2 min, 0% B (100% A) to
248 10% B (90% A) for 2–6 min, 10% B (90% A) to 90% B (10% A) for 1 min, and
249 isocratic 90% B for further 2 min. The flow rate was set at 0.8 mL/min and column
250 temperature at 35 °C. Eluents were detected at λ_{ex} = 404 nm and λ_{em} = 618 nm. To

quantify standards, a solution containing 50 nmol/L URO I in 12.5% TCA was prepared using a 1-mM stock solution dissolved in 1 M HCl (Sigma Aldrich). The concentration of the standard was calculated using absorbance at $\lambda = 405$ nm and $\varepsilon = 505 \times 10^3$ L cm^{-1} mol^{-1} [29]. Standard curves were generated by varying the injection volume and integrating the corresponding peaks.

P. falciparum culture

P. falciparum was cultured in O^+ human erythrocytes at 2.5% hematocrit according to a previously described method [30]. The cell-culture medium (CCM) comprised of RPMI 1640 supplemented with 8.8 mM D-glucose, 22 mM HEPES, 208 nM hypoxanthine (Sigma-Aldrich, Missouri, US), 46.1 nM gentamicin, 2.1 g/L AlbuMAX® I, 2.8 mM L-glutamine (Life Technologies, Australia), and 4.2% (v/v) O^+ human serum. Cultures were maintained in flasks filled with 1%O_2/3%CO_2/96%N_2 gas mix, and kept in an orbitally shaking incubator at 50 rpm at 37°C. Culture parasitemias were maintained at between 0.5% and 10%, and checked every one to two days by visualizing Giemsa-stained thin blood smear by microscopy. CCM was changed every one to two days by pelleting infected cells at 500x*g* for 5 minutes and suspending them in fresh CCM. Human erythrocytes and sera were provided by the Australian Red Cross Blood Service. Blood was washed thrice using CCM that lacked hypoxanthine, AlbuMAX® I, and human serum, and centrifuged at 2800 RPM for 5 minutes after each wash. The *P. falciparum* strain 3D7 was donated by R. Anders (La Trobe University, Melbourne, Australia). The Pf*Pbgd*-KO and 3D7 wild-type parental lines were gifts from Professor Daniel E. Goldberg, Washington University School of Medicine, St. Louis, MO.

276 **TUNEL staining and immunofluorescence**

277 Deoxyuridine triphosphate nick-end labeling by the terminal deoxynucleotidyl
278 transferase (TUNEL) labels degraded or sheared DNA, revealing parasite apoptosis
279 or necrosis. TUNEL and cell staining for immunofluorescence microscopy were
280 performed on blood smears from mice infected with *P. chabaudi* infected mice as
281 described [31], but with some modifications. Mouse blood samples were fixed for at
282 least 24 h in Cytofix solution (BD Biosciences) diluted fourfold in PBS. Slides coated
283 with polyethylenimine (0.1% v/v in PBS) were smeared with fixed blood and stained
284 overnight in the reaction mix from the Apo BrdU TUNEL Assay Kit (Molecular
285 Probes, Eugene, OR). TUNEL-labeled DNA was detected using a biotinylated anti-
286 BrdU antibody and streptavidin-Alexa Fluor 594 conjugate (ThermoFisher Scientific,
287 Australia). At least 100 infected cells were counted on each slide. After staining,
288 slides were mounted in SlowFade™ Gold Antifade Mountant with DAPI
289 (ThermoFisher Scientific, Australia) and glass coverslips (#1 from Menzel-Gläser).
290 Slides were examined at room temperature using an inverted Axio Observer
291 fluorescence microscope or a LSM 800 confocal microscope with Airyscan, both
292 using 630× magnification and coupled to a Axiocam 503 monochrome cameras
293 (Zeiss, Australia). All acquired images were acquired and processed by using the
294 Zeiss Zen lite microscope software (Zeiss, Australia).

295

296 **Immunoblotting**

297 For the mouse studies, proteins were extracted by homogenization of collected tissues
298 and cells in denaturing sodium dodecyl sulfate (SDS) sample buffer (ThermoFisher
299 Scientific, Australia) and clarified by centrifugation. Human erythrocyte membranes
300 were prepared by lysis of uninfected cells in ice-cold 2.5 mM PBS (pH 7.4)

containing cOmplete™ Protease Inhibitors (Roche, Australia), followed by centrifugation (12,000×*g*, 10 min) and washing in the same buffer. Purified parasite samples were prepared from *P. falciparum* cultured in normal erythrocytes and enriched by Percoll density-gradient centrifugation [32]. Parasitized cells were washed in PBS, treated with 0.15% saponin (10× parasite pellet volume) for 10 min, and the released parasites then washed twice in cold PBS containing protease inhibitors and lysed in RIPA lysis buffer (Sigma Aldrich, Australia). Soluble and insoluble fractions of the parasite lysate were recovered after centrifugation (12,000×*g*, 10 min) and analyzed separately. The later fraction consisted mostly of insoluble hemazoin. All samples were mixed with denaturing SDS sample buffer and subjected to SDS-PAGE using 8% gradient gels [33]. Gels were blotted onto membranes. The antibodies used for immunoblotting experiments included rabbit anti-human PBGD IgG from Sigma Aldrich (HPA006114) or from Fitzgerald Industries International (70R-3343) for the murine tissue sample studies, and mouse anti-human PBGD IgG_1 monoclonal antibody from Santa Cruz Biotechnology (sc-271585) and an *N*-terminal Ank-1 ‘‘p89’’ antibody (kindly provided by Connie Birkenmeier, Jackson Laboratory, USA) for human and *P. falciparum* cell studies. Following blotting with HRP-conjugated secondary antibodies (Sigma Aldrich), protein bands were visualized by imaging chemiluminescent (SuperSignal West Pico Substrate, ThermoFisher Scientific).

Generation of PbA_pbgd parasite knockout.

PBGD *P. falciparum* 3D7 sequence was blasted to *P. berghei* ANKA (PbA) genome to retrieve the targeted sequence. To generate the *Pbgd* targeting plasmid, p35/EF5′.K^+GFP.CAM3′ was modified [34] by replacing the K^+GFP sequence with

326 firefly luciferase, yielding the vector p35/EF5′.FF.CAM3′. The 500 bp 5′ flanking
327 sequence of *PbA_pbgd* (PbANKA_060800) was amplified by PCR using the primers
328 PbA_060800/5′FIF (5′-gacccgcggGATCATTATGGCAAATATTCTGCC) and
329 PbA_060800/5′FIR (5′ gacctgcagTATTGCTATAACTATATTATTCAGTTA),
330 digested with *Sac*II and *Pst*I enzymes and cloned into the corresponding sites of
331 p35/EF5′.FF.CAM3′ to generate p35/5'Fl/EF5′.FF.CAM3′. For the 3' homology
332 arm, the 3′ flanking sequence of *PbA_pbgd* was amplified by PCR using the primers
333 PbA_060800/3′FIF (5′-gacgatatcGGATGAGGCAGCTTTATATTACA) and
334 PbA_060800/3′FIR (5′gacgaattcGTTCAAATCGCGTATTTGAATGTGATGTG),
335 digested with *Eco*RV and *Eco*RI and cloned into the corresponding sites of
336 p35/5'Fl/EF5′.FF.CAM3′ to generate p35/5+3'Fl/EF5′.FF.CAM3′. The plasmid
337 vector (1 µg) was then linearized with *Sac*II/*Eco*RI and transfected into PbANKA
338 parasites using previously established methods [35]. The transfected parasites were
339 inoculated into a BALB/c naïve mouse by intravenous inoculation and selected for by
340 administering pyrimethamine into the mouse's drinking water (0.07 mg/mL) for six
341 days. Parasite DNA was extracted and a PCR was conducted to check for successful
342 integration using the following primers PbA_060800_int_F (5′-
343 ATCCGAGCAATATTATCGACAG), hDHFR_R_int (5′-GATGCAGTTTAGCGA-
344 ACCAAC), CAM3'_F_int (5′-GTAAAGGGTTAATTCTTATATGGTC) and
345 Pb060800_int_R (5′-CCATTTTCTCAATACTTACATAG) (Supplementary Figure
346 3). The *PbA_pbgd* parasite was single cloned into 6-8 weeks old BALB/c mice by
347 limiting dilution and verified by PCR according to the procedure described previously
348 [36].
349
350

351 ***P. chabaudi* and *P.berghei* infections**

352 Infection experiments used the rodent parasite *P. chabaudi adami* DS (408XZ) and *P.*
353 *berghei* ANKA. Parasite stocks were prepared by passage through resistant C57BL/6
354 (*P. chabaudi*) or BALB/c (*P. berghei*) mice as described previously [37].
355 Experimental mice were infected by IP injection with a dose of 1×10^4 parasitized
356 erythrocytes. Blood-stage parasitemia was determined by microscopically examining
357 thin blood smears obtained by tail bleeding (1 µL per day from days seven to 14 after
358 infection) and staining with 10% Giemsa solution. Percentages of infected
359 erythrocytes were calculated from a minimum of 1,000 erythrocytes counted.
360
361 **Study subjects**
362 We studied erythrocytes obtained from seven Italian Caucasian AIP patients recruited
363 at the Department of General Medicine, Fondazione IRCC Ca' Granda, Ospedale
364 Maggiore Policlinico, Milan, Italy. All patients had a confirmed biochemical and
365 genetic diagnosis: three patients were asymptomatic carriers and four experienced
366 typical acute attacks. (Table S1).
367
368 **Collection and preparation of purified erythrocytes**
369 Blood from patients with AIP and Italian healthy control subjects was collected by
370 venepuncture into 5-mL tubes containing EDTA. Blood was shipped at 4°C within
371 seven days of collection from the Ospedale Maggiore Policlinico, Milan, Italy to The
372 Australian National University, Canberra, Australia. To purify erythrocytes, samples
373 were centrifuged (170×*g*, 13 min), and plasma and white-cell fractions removed. The
374 remaining erythrocytes were washed twice in RPMI. Erythrocytes were stored at 4°C

for up to one further week before being infected with parasites. Matched normal control samples were shipped, purified, and stored similarly to experimental samples.

P. falciparum growth-inhibition assays

For growth assays, parasites were propagated in normal erythrocytes (from the Australian Red Cross Blood Service), purified using Percoll density-gradient centrifugation [32], and then added to test erythrocytes at a final parasitemia of ~1%. Parasitemias and parasite development stages were determined after culturing for up to 72 h using Giemsa-stained thin blood smears. Growth assays were conducted in duplicate or triplicate for each patient sample unless indicated otherwise. At least 1000 cells were counted on each slide. In some experiments, parasite growth was quantified by flow cytometry after staining culture samples (fixed in Cytofix solution) with 5 µg/mL Hoechst 33342 for 5 min. Fluorescence signals were measured using an LSR Fortessa cell analyzer (BD Biosciences). At least 100,000 events were recorded per sample. BD FACS software was used to process and analyze the data.

Statistical analysis

For malaria survival, statistical significance was determined using the Mantel–Cox test. For other results, two-tailed Students *t*-test was used. A $P < 0.05$ was considered significant

RESULTS

Through out large-scale ENU mutagenesis screen for abnormal red blood cell count, we discovered the *Pbgd*^{MRI58155} mice displaying microcytosis, accompanied by moderately elevated reticulocyte counts, reduced hematocrit and total hemoglobin, but with normal mean erythrocytic hemoglobin levels. We confirmed that the phenotype was heritable after crossing the G1 animal with SJL/J mice and observing that the G1 microcytosis phenotype was passed on to approximately half the offspring. Intercrossing two affected G2 mice produced the wild-type phenotype in approximately one third of the progeny and the G1 founder phenotype in the other two thirds (Table S2). Collectively this indicated a fully penetrant dominant inheritance of the microcytotic phenotype (i.e., heterozygous for the MRI58155 allele) but embryonic lethality in homozygotes.

Whole-exome sequencing of two heterozygous G3 mice and subsequent segregation analysis of mutations in candidate genes identified a single base substitution (A to G) in chromosome 9 (Chr9 44341074, mm10), which is located in the murine *Pbgd* gene (NM_013551). This mutation, designated *Pbgd*^{MRI58155}, is predicted to disrupt splicing of exon 6 and results in a truncated protein comprising 90 amino acids; this protein lacks all conserved residues and domains required for catalytic function of PBGD (Figure 1A).

The mutation completely segregated with the microcytic phenotype over more than 10 generations of breeding. Compared to wild-type mice, reduced amounts of PBGD were observed in immunoblots of proteins extracted from spleen, liver, bone marrow, and erythrocytes from heterozygous mice; furthermore the truncated protein encoded by *Pbgd*^{MRI58155} was not detectable (Figure S1A and S1B). PBGD activity was significantly lower in heterozygous than in wild-type erythrocytes (30.5 ± 2.2 versus

425 39.5 ± 3.5 nkat/L; p = 0.048, (Figure 1B). Urine from heterozygous mice appeared
426 slightly pink. The heterozygous mice exhibited also modest splenomegaly, but normal
427 liver size, and normal iron content in both organs; serum cytokine levels were also
428 similar to those in wild-type mice (Tables S3 and S4). Erythrocyte life span (Figure
429 S2A) and osmotic fragility (Figure S2B) were unaffected by the mutation. In addition,
430 production of erythroid progenitors was also unaffected (Figure S2C).
431
432 To further investigate if the *Pbgd*^{MRI58155} mutation affects the host response to
433 malarial infection, cohorts of heterozygous and wild-type mice were inoculated with
434 *P. chabaudi adami* DS, which is typically lethal to this parental mouse strain (SJL/J).
435 We observed a significantly altered course of infection in heterozygotes compared to
436 wild-type mice. Parasitemias were lower than in wild-type mice between days seven
437 and 10 in female mice (Figure 2A), and days nine and 10 in male mice (Figure 2B). A
438 modest but significant survival advantage was observed for female heterozygotes (p =
439 0.00016); 90% of these animals survived for at least one day longer than their wild-
440 type littermates, although 11 of 12 heterozygous mice eventually succumbed (Figure
441 2C). Two of 21 heterozygous male mice survived the infection, although this was not
442 statistically significant (Figure 2D).
443 We investigated whether the reduced parasitemia observed in the heterozygous mice
444 was due to compromised merozoite capacity to invade erythrocytes. To assess
445 merozoite invasion, we used an *in vivo* erythrocyte-tracking assay (IVET) [37], in
446 which mixtures of distinctly labeled heterozygous and wild-type erythrocytes were
447 transfused into recipient wild-type mice infected with *P. chabaudi*, and the
448 percentages of transferred erythrocytes that became infected determined. Following
449 injection of the labeled erythrocytes into the recipient at the point of parasite

schizogony, the proportion of newly infected erythrocytes measured during the next 30 min to 20 h were similar between the two donor types. After 39 h, the percentage of infected cells had increased, reflecting a second schizogony and infection cycle, but were still similar comparing wild-type and heterozygous cells (Figure 2E). Overall, no significant differences were observed between heterozygous and wild-type cells at any of the tested time points. These results indicate that the heterozygous erythrocytes' susceptibility to merozoite invasion is equal to their wild-type counterparts. We then investigated if the ability of the *P. chabaudi* parasites to grow within erythrocytes was affected by PBGD insufficiency. Thus, we determined the numbers of dead or dying intraerythrocytic *P. chabaudi* in infected heterozygous or wild-type mice using TUNEL [31]. The mean percentages (± SEM) of TUNEL-labeled parasites measured in samples collected 8 and 9 days after infection were 9.0 ± 1.0 and 12.6 ± 1.2 in wild-type mice and 10.4 ± 1.4 and 15.8 ± 1.7 in heterozygous mice; the heterozygous values were significantly greater than those of the wild-type mice at both time points ($p < 0.05$; Figure 2F). This finding suggests that in heterozygous erythrocytes, a greater proportion of parasites are dying, in turn reducing production of new, viable parasites and explaining the observed reduced parasitemia and relatively better survival.

PBGD deficiency in humans can manifest as AIP (MIM 176000). AIP is characterized by occasional, acute episodes of gastrointestinal and neuropathic symptoms; between episodes, the patient is healthy. Acute attacks result from high urinary excretion of the heme precursors, especially δ-aminolevulinic acid and porphobilinogen [38]. We obtained blood samples from seven AIP patients, all with confirmed *PBGD* gene mutations and reduced PBGD activity except for the patient

476 A. Four patients reported a typical history of episodes of acute symptoms with
477 elevated urinary δ-aminolevulinic acid and porphobilinogen levels but were not
478 symptomatic at the time of blood collection (Table 1 and Table S1).
479
480
481 Erythrocytes isolated from these AIP samples and from healthy individuals, all shipped
482 from Italy (hemochromatosis (HC) Italy, n = 2), and from the Australian Red Cross
483 Blood Service (HC Australia, n = 1), were infected with growth-stage-synchronized *P.*
484 *falciparum* (pigmented trophozoites and schizonts). Cultures were incubated for up to
485 72 h and sampled at different time points to count the number of parasitized cells,
486 determine parasite development stages, and compare parasite propagation and their
487 intraerythrocytic development, over time. Following the first 24 h of culturing, when
488 parasite had egressed from donor erythrocytes and invaded the surrounding test cells,
489 we observed no differences in parasitemia fold-change (Figure 3A Normal ARC and
490 Normal Italy). After 72 h, while parasites had replicated in test erythrocytes and
491 undergone a further cycle of schizogony and cell invasion but the number of parasitized
492 erythrocytes in the HC and AIP samples were in similar proportion to 3D7 *P.*
493 *falciparum* samples. Collectively, these results indicate that the *P. falciparum* could
494 normally infect the AIP erythrocytes and establish within them without their
495 intraerythrocytic growth being affected. A *P. falciparum* clone carrying a genetic
496 disruption of the parasite *Pbgd* homolog (PF3D7_1209600) was shown previously to
497 grow as well as its wild-type parent strain (3D7) in normal human erythrocytes [14].
498 We obtained these lines (designated here as Pf*Pbgd*-KO and 3D7) and compared their
499 growth characteristics using the same parasite-culturing approach described above.
500 Two normal erythrocyte samples (HC Australia and HC Italy) and six AIP erythrocyte
501 samples (from AIP patients with mutation types A, B, C, and D) were tested. Both

parasite lines cultured in the HC erythrocytes established similar parasitemia levels and increased more than six-fold after 72 h. When the two lines were cultured in AIP erythrocytes, the growth of Pf*Pbgd*-KO parasites was comparable to the 3D7 parasites (Figure 3A).

Given the intraerythrocytic growth defect seen in *P. chabaudi* infection, we investigated whether the intraerythrocytic maturation of the parasite during *P. berghei* infection was also affected. We generated a homologue Pbgd-deficient parasite in *P. berghei ANKA* (PbA_060800) (Figure S2). Similarly to the *P. falciparum* ortholog, the parasite developed normally along the erythrocytic stage of parasitic maturation during *P. berghei* infection (Figure 3B) (named thereafter PbA_pbgd). We examined whether PbA_pbgd erythrocytic maturation is affected in $Pbgd^{MRI58155/+}$ mice. We noted comparable parasitemia in Pb_ANKA infection between wild-type or $Pbgd^{MRI58155/+}$ mice. However we observed a slight difference in parasitemia between PbA_Pbgd and Pb_ANKA in SJL/J background at day 11 days after inoculation. Importantly we noted no differences in parasitemia between PbA_Pbgd and Pb_ANKA in $Pbgd^{MRI58155/+}$ mouse during the course of the infection but a slight increase in survival for these mice at day 17 post-inoculation. Therefore, while deletion of parasite *Pbgd* gene did not affect its ability to grow in normal erythrocytes, which confirms a previous study [14], as is consistent with the *P. falciparum* results above, the growth of *P. chabaudi* in contrast was perturbed in host erythrocytes. Together this might indicate that while the requirement of host PBGD of *Plasmodium* is not formally ruled out, these results might suggest that the resistance to *P. chabaudi* infection in PBGD deplete mice could be also due to an effect not directly linked to PBGD deficiency.

DISCUSSION

Here, we describe the identification and characterization of an ENU-induced mutation in the murine *Pbgd* gene (*Pbgd*^{MRI58155}). Mice heterozygous for this mutation display a relatively normal phenotype, distinguished by microcytosis and a modest, but significant decrease in erythrocytic PBGD activity, although they exhibited no overt symptoms characteristic symptoms of AIP. Previous studies showed that a profound deficiency of PBGD in mice is necessary in mice to mimic human AIP [39]. The protein expressed by the *Pbgd*^{MRI58155} allele is predicted to be truncated and completely inactive, and consistent with this prediction, we could never obtained homozygous pups. However, rather than the predicted 50% reduction in enzyme activity, heterozygotes retained ~75% of normal enzyme activity in their blood. Possibly a partially functional protein is expressed by the mutant allele, or expression by the wild-type allele is compensatorily increased. The most prominent consequence of the *Pbgd*^{MRI58155} mutation, and indeed the phenotypic basis of its identity, was a modest microcytic anemia, although erythrocyte number and erythrocytic hemoglobin concentrations were normal. Reduced biosynthesis of heme in erythroid progenitors can often lead to generation of microcytic anemia, although this is not characteristic of human AIP, and is not a reported effect for the *Pbgd*-null or hypomorphic mutations [39]. However, microcytic erythrocytes have been observed in cats with *Pbgd* mutations displaying AIP symptoms [40]. Overall, the *Pbgd*^{MRI58155} allele results in a phenotype consistent with a mild, asymptomatic form of AIP.

We used the *Pbgd*^{MRI58155} mouse line, as well as erythrocytes from AIP patients with PBGD deficiency to investigate potential dependence of *Plasmodium* on the host enzyme for its growth and survival. These studies were motivated by previous observations that other host heme biosynthetic enzymes are co-opted by the parasite

554 and that they may be potential antimalarial therapeutic targets [5, 9, 11, 15, 19]. We
555 found that *P. chabaudi* growth was modestly perturbed in mice but not in *P. berghei*
556 infected mice and human erythrocytes with reduced PBGD levels. This was
557 evidenced by reduced parasite propagation, increased intraerythrocytic parasite death,
558 and modest but significant protection against *P. chabaudi* infection in the
559 $Pbgd^{MRI58155}$ mutant mice. Our experiments using mice and analysis of parasite
560 development in the AIP erythrocytes demonstrated that invasion of mutant
561 erythrocytes by wild-type merozoites was not inhibited. We also excluded other
562 possible indirect effects of the enzyme deficiency in the mouse, including their
563 cellular hemoglobin levels, relevant indices of which were relatively normal. We
564 therefore propose that the reason parasite *P. chabaudi* growth was impaired in mutant
565 mice is because that *Plasmodium* has a certain requirement for host PBGD. This
566 hypothesis was not supported by our observation that parasites lacking their own
567 version of *Pbgd* grew similarly to wild-type counterparts in AIP erythrocytes with the
568 *Pbgd* hypomorphic mouse mutation. It is possible the parasite requires a certain
569 threshold level of enzyme to grow, a proportion of which is likely contributed from
570 by erythrocytes; the parasitic growth defect is only manifested in host cells with
571 highly reduced PBGD levels, which was not observed in our AIP samples and *Pbgd*-
572 deficient mouse line. It is also possible that the parasite requires precursors of the
573 heme biosynthetic pathway, which may be produced by infected host cells [14].
574

575 **CONCLUSIONS**

576 Our data indicate that *Plasmodium berghei* or *Plasmodium falciparum* but not
577 *Plasmodium chabaudi* do not require erythrocytic PBGD for its growth and
578 propagation in erythrocytes and the parasite PBGD homolog is dispensable

compatible with the possibility that the resistance to *P. chabaudi* of PBGD deplete mice erythrocytes is probably not due to the direct effect of Pbgd mutation. However our data does not exclude the possibility of a requirement of the host PBGD to the parasite as the depleted host PBGD possessed a sufficient enzyme activity to compensate the loss of parasite PBGD. An interesting investigation to further explore this question would be to test specific small-molecule inhibitors for PBGD, which have been developed [41] but would require the synthesis of these as they are unfortunately currently unavailable to test. This would then elucidate the role of host PBGD during malaria infection and whether our hypothesis of a certain requirement of the enzyme by the parasite can be confirmed.

LIST OF ABBREVIATIONS

AIP: acute intermediate porphyria

CCM: cell-culture medium

ENU: N-ethyl-N-Nitrosourea

FC: Ferrochelatase

HC: Hemochromatosis

IP: intraperitoneally

Pb_A: *Plasmodium berghei* ANKA

PBGD: porphobilinogen deaminase

PBS: phosphate-buffered saline

RBC(s): erythrocyte(s)

SDS: sodium dodecyl sulfate

TCA: trichloroacetic acid

UHPLC: ultrahigh-performance liquid chromatography

URO: uroporphyrinogen

TUNEL: Terminal deoxynucleotidyl transferase dUTP nick-end labeling

DECLARATIONS

Ethics approval and consent to participate:

Blood sampling and experimental procedures involving patients were performed in accordance with the 1983 revision of the Declaration of Helsinki. The study was approved by the Ethical Committee of Fondazione IRCCS Ca' Granda, Ospedale Maggiore Policlinico, Milan, Italy (Project Number 246_2015) and The Australian National University Human Research Ethics Committee (2014/765).

All procedures involving animals conformed to the *Australian code of practice for the care and use of animals for scientific purposes* by the Australian National Health and Medical Research Council and were approved by the Macquarie University Animal Ethics Committee (Project Numbers: ARA 2012/017 and 2012/019), the Australian National University Animal Experimentation Ethics Committee (2014/53) and Deakin University animal ethics committee (Project Number G37-2013).

Consent for publication:

Not applicable

Availability of data and materials:

All data generated or analyzed during this study are included in this published article and its supplementary information files.

631

632 **Competing interests.**

633 The authors declare that they have no competing interest to disclose.

634

635 **Funding:**

636 The Authors were supported by an International Macquarie University Research
637 Excellence Scholarship (CBS), the NHMRC (490037, 605524, APP1047090 and
638 APP1066502), the Australian Research Council (DP120100061) and the National
639 Collaborative Research Infrastructure (NCRIS) via the Australian Phenomics
640 Network (APN). Funders had no role in the design of the study and collection,
641 analysis, and interpretation of data or in writing the manuscript.

642

643 **Author Contributions**

644 CBS, HY, LS, AE, TKW, FR, and BJM performed experiments and DCB analyzed
645 the exome sequencing data. The project was conceived by BJM, GB and SJF and
646 experiments were designed by CBS, HY, BJM and GB. The blood samples, and the
647 genetic and biochemical analysis of the AIP patients were provided and performed by
648 EDP and GG. The paper was written and the figures were prepared by CBS, EDP,
649 GG, GB and BJM. All authors read and approved the final manuscript.

650

651 **ACKNOWLEDGEMENTS**

652 We thank Ceri Flowers for administrative support, Diana Spinelli for recruitment of
653 the AIP patients, Shelley Lampkin for technical assistance, Elinor Hortle for assisting
654 with the cytokine assays, Gavin Symonds and Zeiss Australia for confocal imaging
655 analysis, and the Australian Red Cross Blood Service for red cells and human serum.

656

657

658 **REFERENCES**

659 1. Allison, A.C., *Genetic control of resistance to human malaria.* Curr Opin
660 Immunol, 2009. **21**(5): p. 499-505.
661 2. Hill, A.V., *The immunogenetics of resistance to malaria.* Proc Assoc Am
662 Physicians, 1999. **111**(4): p. 272-7.
663 3. Min-Oo, G. and P. Gros, *Erythrocyte variants and the nature of their malaria*
664 *protective effect.* Cell Microbiol, 2005. **7**(6): p. 753-63.
665 4. Nagel, R.L. and E.F. Roth, Jr., *Malaria and red cell genetic defects.* Blood,
666 1989. **74**(4): p. 1213-21.
667 5. Bonday, Z.Q., et al., *Import of host delta-aminolevulinate dehydratase into the*
668 *malarial parasite: identification of a new drug target.* Nat Med, 2000. **6**(8): p.
669 898-903.
670 6. Dhanasekaran, S., et al., *Delta-aminolevulinic acid dehydratase from*
671 *Plasmodium falciparum: indigenous versus imported.* J Biol Chem, 2004.
672 **279**(8): p. 6934-42.
673 7. Koncarevic, S., et al., *The malarial parasite Plasmodium falciparum imports*
674 *the human protein peroxiredoxin 2 for peroxide detoxification.* Proc Natl
675 Acad Sci U S A, 2009. **106**(32): p. 13323-8.
676 8. Sicard, A., et al., *Activation of a PAK-MEK signalling pathway in malaria*
677 *parasite-infected erythrocytes.* Cell Microbiol, 2011. **13**(6): p. 836-45.
678 9. Varadharajan, S., et al., *Localization of ferrochelatase in Plasmodium*
679 *falciparum.* Biochem J, 2004. **384**(Pt 2): p. 429-36.
680 10. Brizuela, M., et al., *Treatment of erythrocytes with the 2-cys peroxiredoxin*
681 *inhibitor, Conoidin A, prevents the growth of Plasmodium falciparum and*

enhances parasite sensitivity to chloroquine. PLoS One, 2014. **9**(4): p. e92411.

11. Smith, C.M., et al., *Griseofulvin impairs intraerythrocytic growth of Plasmodium falciparum through ferrochelatase inhibition but lacks activity in an experimental human infection study.* Sci Rep, 2017. **7**: p. 41975.

12. Ke, H., et al., *The heme biosynthesis pathway is essential for Plasmodium falciparum development in mosquito stage but not in blood stages.* J Biol Chem, 2014. **289**(50): p. 34827-37.

13. Nagaraj, V.A., et al., *Malaria parasite-synthesized heme is essential in the mosquito and liver stages and complements host heme in the blood stages of infection.* PLoS Pathog, 2013. **9**(8): p. e1003522.

14. Sigala, P.A., et al., *Deconvoluting heme biosynthesis to target blood-stage malaria parasites.* Elife, 2015. **4**.

15. Bonday, Z.Q., et al., *Heme biosynthesis by the malarial parasite. Import of delta-aminolevulinate dehydrase from the host red cell.* J Biol Chem, 1997. **272**(35): p. 21839-46.

16. Pasini, E.M., et al., *In-depth analysis of the membrane and cytosolic proteome of red blood cells.* Blood, 2006. **108**(3): p. 791-801.

17. Pasini, E.M., et al., *Deep-coverage rhesus red blood cell proteome: a first comparison with the human and mouse red blood cell.* Blood Transfus, 2010. **8 Suppl 3**: p. s126-39.

18. Pasini, E.M., et al., *Deep coverage mouse red blood cell proteome: a first comparison with the human red blood cell.* Mol Cell Proteomics, 2008. **7**(7): p. 1317-30.

19. Smith, C.M., et al., *Red cells from ferrochelatase-deficient erythropoietic protoporphyria patients are resistant to growth of malarial parasites.* Blood, 2015. **125**(3): p. 534-41.

20. Chen, K., et al., *Resolving the distinct stages in erythroid differentiation based on dynamic changes in membrane protein expression during erythropoiesis.* Proc Natl Acad Sci U S A, 2009. **106**(41): p. 17413-8.

21. Bauer, D.C., et al., *Genome-wide analysis of chemically induced mutations in mouse in phenotype-driven screens.* BMC Genomics, 2015. **16**(1): p. 866.

22. Li, H. and R. Durbin, *Fast and accurate short read alignment with Burrows-Wheeler transform.* Bioinformatics, 2009. **25**(14): p. 1754-60.

23. Langmead, B. and S.L. Salzberg, *Fast gapped-read alignment with Bowtie 2.* Nat Methods, 2012. **9**(4): p. 357-9.

24. Li, H., et al., *The Sequence Alignment/Map format and SAMtools.* Bioinformatics, 2009. **25**(16): p. 2078-9.

25. McKenna, A., et al., *The Genome Analysis Toolkit: a MapReduce framework for analyzing next-generation DNA sequencing data.* Genome Res, 2010. **20**(9): p. 1297-303.

26. Wang, K., M. Li, and H. Hakonarson, *ANNOVAR: functional annotation of genetic variants from high-throughput sequencing data.* Nucleic Acids Res, 2010. **38**(16): p. e164.

27. Benton, C.M., et al., *Ultra high-performance liquid chromatography of porphyrins in clinical materials: column and mobile phase selection and optimisation.* Biomed Chromatogr, 2012. **26**(6): p. 714-9.

28. Benton, C.M., et al., *Ultra high-performance liquid chromatography of porphyrins.* Biomed Chromatogr, 2012. **26**(3): p. 331-7.

731 29. Erlandsen, E.J., et al., *Determination of porphobilinogen deaminase activity in*
732 *human erythrocytes: pertinent factors in obtaining optimal conditions for*
733 *measurements.* Scand J Clin Lab Invest, 2000. **60**(7): p. 627-34.
734 30. Trager, W. and J.B. Jensen, *Human malaria parasites in continuous culture.*
735 Science, 1976. **193**(4254): p. 673-5.
736 31. McMorran, B.J., et al., *Platelets kill intraerythrocytic malarial parasites and*
737 *mediate survival to infection.* Science, 2009. **323**(5915): p. 797-800.
738 32. Rivadeneira, E.M., M. Wasserman, and C.T. Espinal, *Separation and*
739 *concentration of schizonts of Plasmodium falciparum by Percoll gradients.* J
740 Protozool, 1983. **30**(2): p. 367-70.
741 33. Laemmli, U.K., *Cleavage of structural proteins during the assembly of the*
742 *head of bacteriophage T4.* Nature, 1970. **227**(5259): p. 680-5.
743 34. Haase, S., et al., *The exported protein PbCP1 localises to cleft-like structures*
744 *in the rodent malaria parasite Plasmodium berghei.* PLoS One, 2013. **8**(4): p.
745 e61482.
746 35. Janse, C.J., J. Ramesar, and A.P. Waters, *High-efficiency transfection and*
747 *drug selection of genetically transformed blood stages of the rodent malaria*
748 *parasite Plasmodium berghei.* Nat Protoc, 2006. **1**(1): p. 346-56.
749 36. Janse, C.J., et al., *High efficiency transfection of Plasmodium berghei*
750 *facilitates novel selection procedures.* Mol Biochem Parasitol, 2006. **145**(1):
751 p. 60-70.
752 37. Lelliott, P.M., et al., *A flow cytometric assay to quantify invasion of red blood*
753 *cells by rodent Plasmodium parasites in vivo.* Malar J, 2014. **13**: p. 100.
754 38. Puy, H., L. Gouya, and J.C. Deybach, *Porphyrias.* Lancet, 2010. **375**(9718):
755 p. 924-37.

39. Lindberg, R.L., et al., *Porphobilinogen deaminase deficiency in mice causes a neuropathy resembling that of human hepatic porphyria.* Nat Genet, 1996. **12**(2): p. 195-9.

40. Clavero, S., et al., *Feline acute intermittent porphyria: a phenocopy masquerading as an erythropoietic porphyria due to dominant and recessive hydroxymethylbilane synthase mutations.* Hum Mol Genet, 2010. **19**(4): p. 584-96.

41. Ahmed, R. and F.J. Leeper, *A new synthesis of porphobilinogen analogues, inhibitors of hydroxymethylbilane synthase.* Org Biomol Chem, 2003. **1**(1): p. 21-3.

42. Martinez di Montemuros, F., et al., *Acute intermittent porphyria: heterogeneity of mutations in the hydroxymethylbilane synthase gene in Italy.* Blood Cells Mol Dis, 2001. **27**(6): p. 961-70.

FIGURES LEGENDS:

Figure 1. Analysis of the *Pbgd*^{MRI58155} mutation.

Schematic of the full-length 361 residue murine Pbgd protein, including locations of the three domains and active site residues, R^{25} and S^{28} (sulfate-binding), D^{99} (catalytic), S^{147}, R^{150} and R^{173} (pyrrole-cofactor-interacting) and C^{261} (pyrrole-cofactor-binding), based on a solved human Pbgd crystal structure; Gill et al 2009). The predicted 90 residue Hmbs^{MRI58155} protein is shown below. Its lacks the sequences containing the catalytic domain and cofactor binding sites (**A**). Measurement of Pbgd enzyme activity in whole blood samples from WT and Het mice using HPLC. Data represent the mean (box) and values from four mice per group, each assayed two times. * $P < 0.05$, calculated using a two-tailed *t*-test assuming equal variance (**B**).

Figure 2: Mice with the *Pbgd*^{MRI58155} mutation display an increased resistance to infection with *P. chabaudi*. *Pbgd*^{MRI58155} heterozygotes (Het) and wild-type littermates (WT) were infected with *P. chabaudi* ($1x10^4$ parasites; 13-21 mice per group) and analyzed for percentage of circulating infected erythrocytes (% parasitemia, in females (**A**) and males (**B**), as well as survival in females (**C**) and males (**D**). Eight WT mice infected with *P. chabaudi* were injected intravenously with differently labelled WT and Het blood (day eight post-inoculation) and % parasitemia was determined in each labeled cell type at various time points (**E**). Proportions of TUNEL-labeled parasite-infected erythrocytes in WT and Het mice (five per group) infected with *P. chabaudi* (**F**). Error bars represent SEM. * $p < 0.05$, ** $p < 0.01$, calculated using a two-tailed *t*-test assuming equal variance. Log-rank (Mantel-Cox test) for differences in survival yielded P - 0.0016 (female group) and P = 0.16 (male).

Figure 3. ***Plasmodium growth in erythrocytes from individuals with AIP individuals and in PBGD-deficient mice.***

The seven AIP patient samples assayed for P. falciparum growth. Comparison of *Pbgd* knockout *P. falciparum* (Pf_Pbgd KO) with parental wild-type (WT) growth in AIP and normal erythrocytes (RBCs) with the four different AIP B samples assayed in duplicate at 24 h, and once at 48 h and 72 h (**A**). Comparison of *Pbgd*-knockout *P. berghei* (PbA_Pbgd KO) and parental wild-type (WT) growth in infected WT and $Pbgd^{MRI58155}$ heterozygous mice (**B**) The four different AIP B samples were assayed in duplicate at 24 h, and once at 48 h and 72 h. $Pbgd^{MRI58155}$ heterozygotes (Het) and wild-type littermates (WT) were infected with *P. berghei ANKA* ($1x10^4$ parasites; 8 to 15 mice per group) All other samples samples were assayed in duplicate or triplicate. * $p < 0.05$, ** $p < 0.01$, *** $p < 0.001$, **** $p < 0.0001$ calculated using a two-tailed *t*-test assuming equal variance.

TABLES:

Table 1. AIP patient samples assayed for *P.falciparum* growth assays.

AIP type	PBGD mutation (*PBGD* ID, or novel)	PBGD protein defect (predicted % normal cellular PBGD activity)	Number of patient samples
AIP A	c.[498+93_1086+211del3137];[=] (novel)	p.(Arg167_Ter362del) (50%)	1
AIP B	c.[913-1 G>C];[=] (novel)	p.(His305_Ter362del) (50%)	4
AIP C	c.[580C>T];[=] (H971935)	p.(Gln194Ter) (50%)	1
AIP D	c.[760_763delCTGAinsTCG];[=] (novel)	p.(Leu254Serfster11) (50%)	1

The AIP C mutation (H971935) has been previously described [42].

889 **Figure S1:** Immunoblot analysis of Pbgd protein expression in various tissues from
890 $Pbgd^{+/+}$ (WT) and $Pbgd^{MRI58155/+}$ (Het) mice, using a rabbit anti-human PBGD antibody
891 (Sigma Aldrich) (**A**) and a goat anti-human antibody (**B**). The full-length Pbgd protein is
892 detected at approximately 39 kD. Analyzed tissues included whole blood (WB), bone
893 marrow (BM), spleen (Sp), liver (Lv), and red blood cells (RBC) fractionated into
894 hemoglobin-depleted cell lysate (Lys) and cell membrane (Memb)
895
896 **Figure S2: Hematological analysis of the *Pbgd*^{MRI58155} mouse line.**
897 **A** Comparison of erythrocyte life span, **B** osmotic strength, and **C** bone-marrow erythroid
898 progenitor cells in *Pbgd*^{MRI58155} heterozygotes (Het, n = 6 to 9 mice) and wild-type
899 littermates (WT, n = 6 to 7 mice). Error bars represent SEM. No significant differences
900 were observed between groups using the two-tailed Student's *t*-test assuming equal
901 variance.
902
903 **Figure S3: Generation of *Pbgd P. berghei* knockout.**
904 **A** For targeted gene deletion of the PbANKA_060800, fragments of the 5' UTR and 3'
905 UTR, which would serve as targeting regions to drive integration into the endogenous
906 locus, were PCR-amplified from *P. berghei* ANKA genomic DNA and cloned into the
907 p35/EF5'.Fluc.CAM3' vector. Position of oligonucleotides used for PCR analysis are
908 shown. **B** Representation of a gel electrophoresis on the genomic integration of the
909 targeting construct using specific primers spanning the locus.
910
911

Figure 1

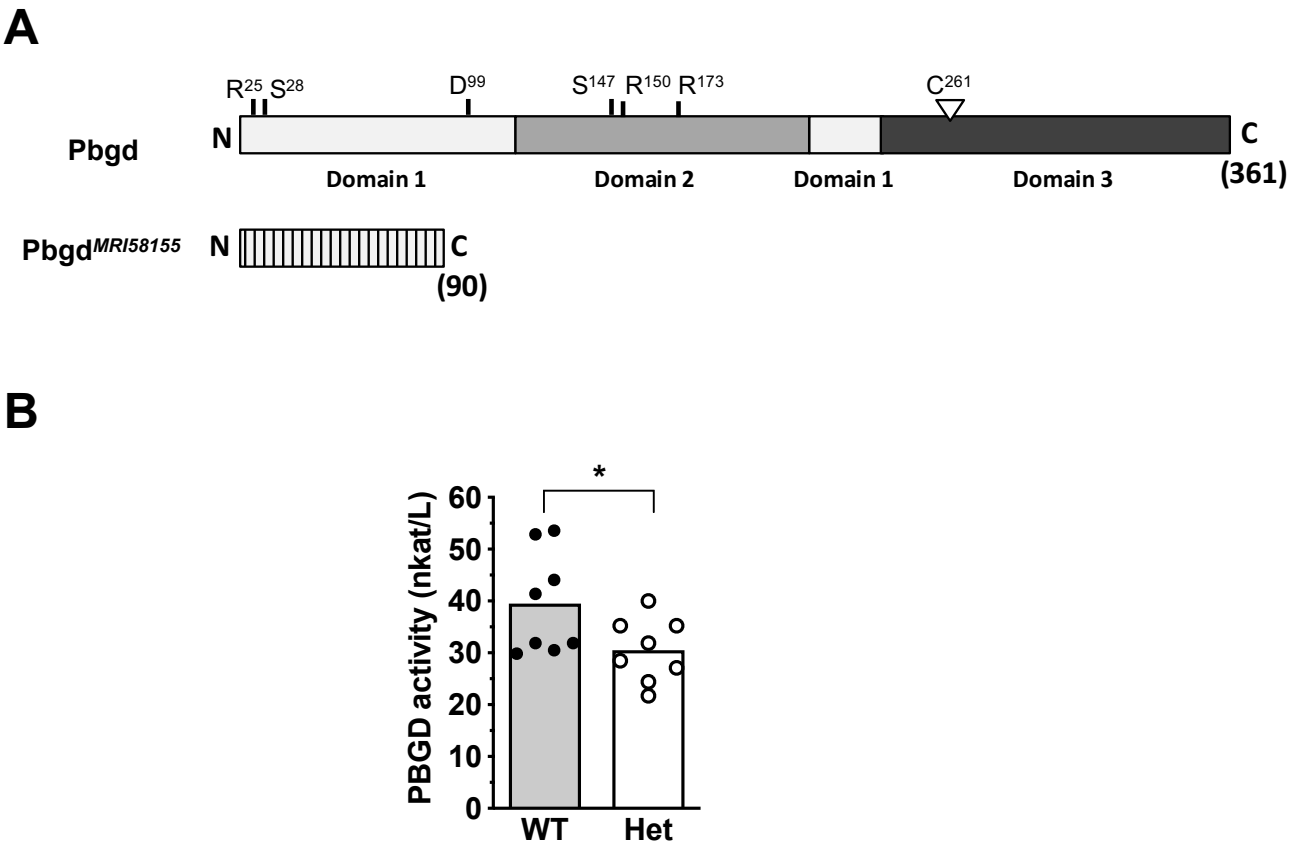

Figure 1. Analysis of the *Pbgd*^{MRI58155} mutation.
Schematic of the full-length 361 residue murine Pbgd protein, including locations of the three domains and active site residues, R^{25} and S^{28} (sulfate-binding), D^{99} (catalytic), S^{147}, R^{150} and R^{173} (pyrrole-cofactor-interacting) and C^{261} (pyrrole-cofactor-binding), based on a solved human Pbgd crystal structure; Gill et al 2009). The predicted 90 residue Hmbs^{MRI58155} protein is shown below. Its lacks the sequences containing the catalytic domain and cofactor binding sites (**A**). Measurement of Pbgd enzyme activity in whole blood samples from WT and Het mice using HPLC. Data represent the mean (box) and values from four mice per group, each assayed two times. * $P < 0.05$, calculated using a two-tailed *t*-test assuming equal variance (**B**).

Figure 2

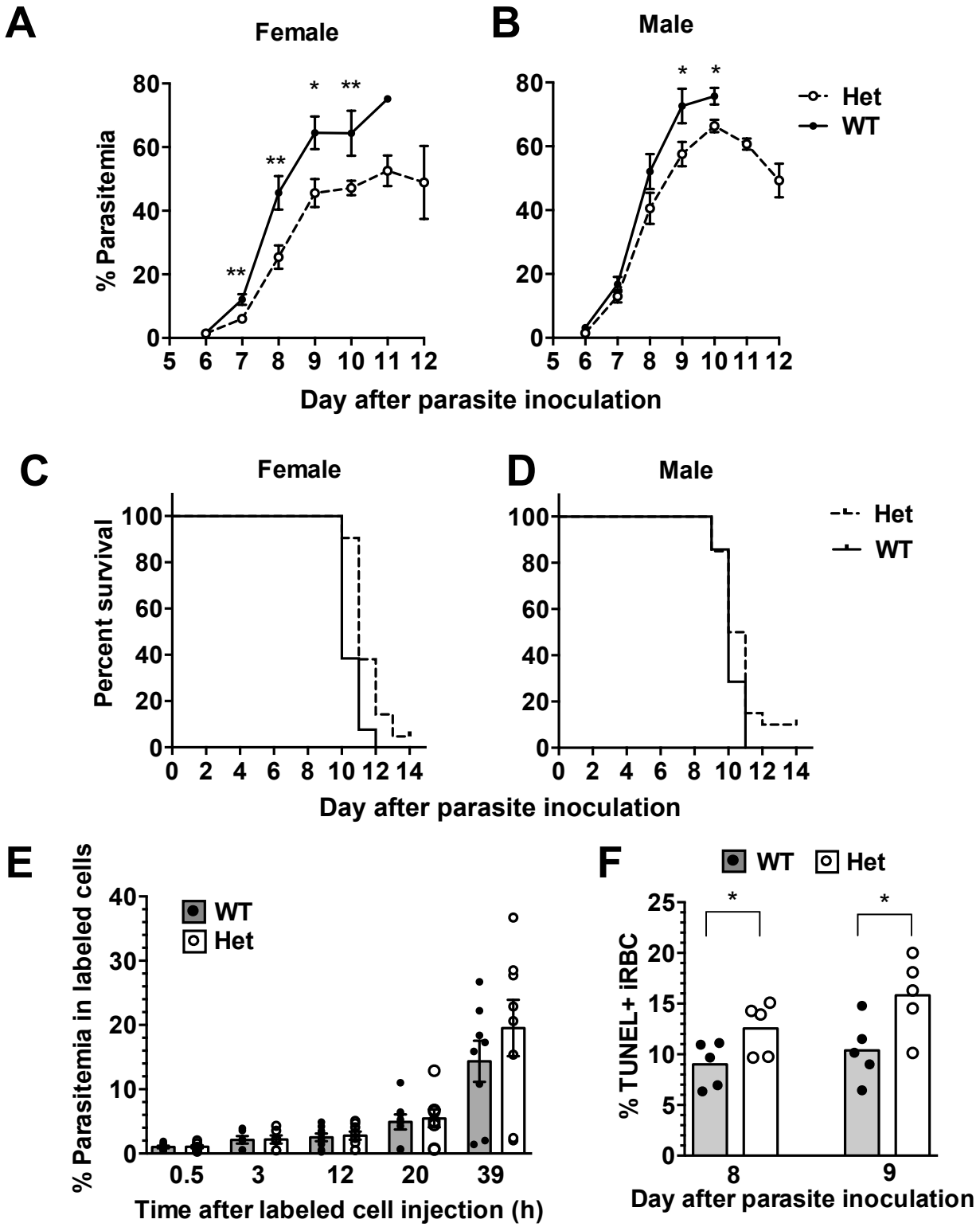

Figure 2: Mice with the *Pbgd*^{MRI58155} mutation display an increased resistance to infection with *P. chabaudi*. *Pbgd*^{MRI58155} heterozygotes (Het) and wild-type littermates (WT) were infected with *P. chabaudi* (1x10^4 parasites; 13-21 mice per group) and analyzed for percentage of circulating infected erythrocytes (% parasitemia, in females (**A**) and males (**B**), as well as survival in females (**C**) and males (**D**). Eight WT mice infected with *P. chabaudi* were injected intravenously with differently labelled WT and Het blood (day eight post-inoculation) and % parasitemia was determined in each labeled cell type at various time points (**E**). Proportions of TUNEL-labeled parasite-infected erythrocytes in WT and Het mice (five per group) infected with *P. chabaudi* (**F**). Error bars represent SEM. * $p < 0.05$, ** $p < 0.01$, calculated using a two-tailed *t*-test assuming equal variance. Log-rank (Mantel-Cox test) for differences in survival yielded P - 0.0016 (female group) and P = 0.16 (male).

Figure 3

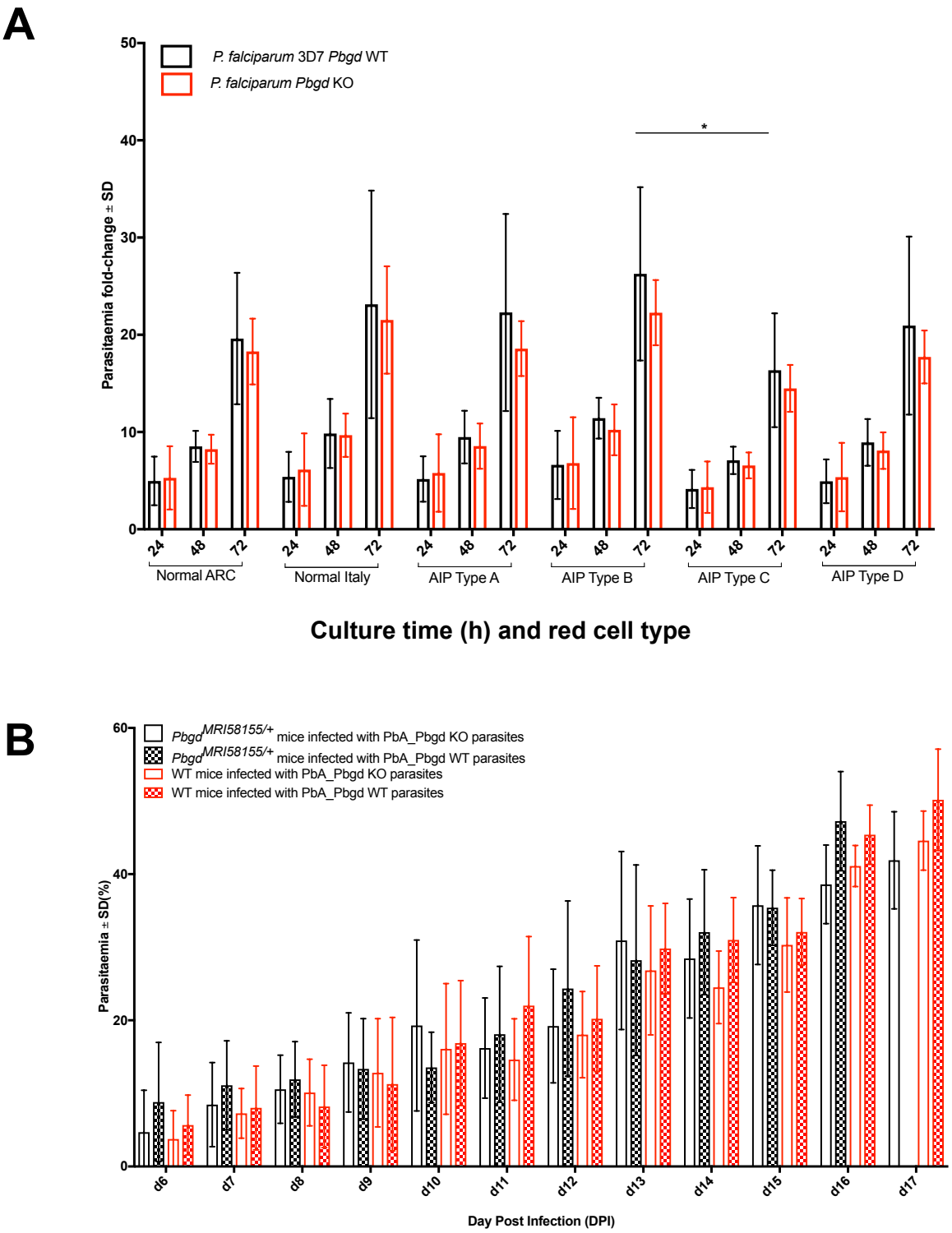

Figure 3. ***Plasmodium growth in erythrocytes from individuals with AIP individuals and in PBGD-deficient mice.***
The seven AIP patient samples assayed for P. falciparum growth. Comparison of *Pbgd* knockout *P. falciparum* (Pf_Pbgd KO) with parental wild-type (WT) growth in AIP and normal erythrocytes (RBCs) with the four different AIP B samples assayed in duplicate at 24 h, and once at 48 h and 72 h (**A**). Comparison of *Pbgd*-knockout *P. berghei* (PbA_Pbgd KO) and parental wild-type (WT) growth in infected WT and $Pbgd^{MRI58155}$ heterozygous mice (**B**) The four different AIP B samples were assayed in duplicate at 24 h, and once at 48 h and 72 h. $Pbgd^{MRI58155}$ heterozygotes (Het) and wild-type littermates (WT) were infected with *P. berghei ANKA* ($1x10^4$ parasites; 8 to 15 mice per group) All other samples samples were assayed in duplicate or triplicate. * $p < 0.05$, ** $p < 0.01$, *** $p < 0.001$, **** $p < 0.0001$ calculated using a two-tailed *t*-test assuming equal variance.